

EXPERIMENTAL AND THEORETICAL STUDIES OF LARGE AMPLITUDE SHIP ROLLING AND CAPSIZE

B. Cotton¹ & K.J. Spyrou²

¹ Centre for Nonlinear Dynamics and its Applications, University College London, UK
(b.cotton@ucl.ac.uk)

² Ship Design Laboratory, National Technical University of Athens, Greece
(spyrou@deslab.ntua.gr)

ABSTRACT

In this paper we are dealing with two different, yet closely connected, problems: Firstly, we propose a new method for deriving the equivalent linear damping which takes into account the dynamics of ship rolling up to very large angles. This new equivalent damping can be introduced into the simple design formula proposed by Thompson in order to achieve a better prediction of capsizing at the initial design stage. Secondly, we present the results from a series of experiments recently carried out at UCL focusing on large amplitude rolling and capsizing. The experimentally derived capsizing boundary is compared with the theoretical one with promising results.

1. INTRODUCTION

Ensuring that a ship can resist capsizing when confronted with steep waves is an important consideration during design. However, current ship design practices take little account of the well-established nonlinear character of the large-amplitude rolling responses which are known to occur in such an environment. An interesting recent development was the proposal by Thompson [1] of a simple design formula which can take into account the strongly nonlinear character of the restoring curve. This formula is a good first step for the initial design stage where an approximate value of the required, for capsizing avoidance, level of damping is sought. However, the formula is derived with the assumption of linear damping which is inconvenient given the well-known existence of a quadratic or cubic type nonlinearity in this term. In order to be able to use the design formula of Thompson and still take into account the nonlinearity of damping, we have developed a new technique of equivalent

damping linearisation which fully takes into account the behaviour near capsizes. This new technique is discussed in Section 2.

Another problem that we analyse in this paper is the experimental verification of the theory of ship capsizes based on nonlinear dynamics. In recent years we have seen many applications of this theory which have greatly enhanced our understanding of the capsizing process [1-3]. It has been shown, for example, that due to the severe nonlinearity of the GZ curve in the region around resonance, multiple steady-state roll responses can emerge, which can undergo further complicated qualitative changes of their character. More complex still can be the transient motions near to capsizing limits. Although theoretical models have been studied to considerable depth with various computational techniques, there has been much less activity in the experimental field especially concerning the agreement of theoretical and experimental results. Some of the problems that exist in carrying out capsizing experiments were summarised in [4]. Well known earlier experimental efforts have been those described in [5] and more recently in [6]. In Section 3 we describe a series of model experiments recently carried out at UCL with the main objective of replicating some of the results seen in numerical investigations. We focus on the comparison between the experimental capsizing boundary and the prediction of nonlinear dynamics. We have used a simple prismatic-type model which was derived from a transverse section of the model originally used in [5].

We present firstly the resonance response diagram obtained, which with a bistable region, clearly displays the nonlinear nature of the system. We also discuss how the robustness of the two possible roll motions demonstrates the need to consider such behaviour in any study of large angle roll. The results of a set of transient capsizing tests are then compared to predictions obtained by numerically integrating the single degree of freedom roll equation. One important conclusion based on the tests is that the real capsizing boundary is much nearer to the boundary predicted for a system with asymmetric restoring in spite of the initial 'symmetry' of the model in calm water. The existence of wave induced bias and its implications for modelling capsizes are discussed with reference to the experimental evidence.

3. A NEW EQUIVALENT LINEAR DAMPING FOR CAPSIZING

The search for some 'equivalent' linear system of ship rolling in regular as well as in irregular seas has been pursued several times in the past [7, 8, 9]. A very popular method to derive the equivalent linear damping is on the basis of an energy balance approach, where we request that the dissipated energy per cycle to be the same for the linear and the nonlinear system. The additional requirement in our case however is that we have to make sure that the behaviour near capsizing is taken into account. Let's consider the following roll model,

$$(I + \Delta I)\theta'' + B(\theta') + mg GZ(\theta) = I Ak \omega_f^2 \sin(\omega_f \tau) \quad (1)$$

where the prime denotes differentiation with respect to real (unscaled) time, τ , θ is the roll angle relative to the wave normal, $B(\theta')$ is the nonlinear damping function,

$GZ(\theta)$ is the roll restoring force, Ak is the wave slope amplitude (A is the wave height and k the wave number) and ω_f is the wave frequency. We also write ω_n , as the linearised natural frequency of undamped motions. By nondimensionalising we obtain:

$$\ddot{x} + b(\dot{x}) + c(x) = F \sin(\omega t) \quad (2)$$

where $x = \theta / \theta_v$ is the scaled roll angle, $\omega = \omega_f / \omega_n$ and a dot denotes differentiation with respect to the scaled time $t = \omega \tau$. Note that this scaling ensures that nondimensional angle of vanishing stability is always equal to 1. The nondimensional nonlinear damping $b(\dot{x})$ depends on some number of parameters b_1, \dots, b_n and,

$$b(\dot{x}) = \frac{B(\dot{x}\theta_v\omega_n)}{\theta_v mgGM} \quad c(x) = \frac{GZ(x\theta_v)}{\theta_v GM} \quad F = \frac{IAk\omega^2}{(I + \Delta I)\theta_v} \quad (3)$$

We then consider an 'equivalent' (only in respect to the amount of dissipated energy) system whose coefficient ζ remains to be identified,

$$\ddot{x} + 2\zeta\dot{x} + c(x) = F \sin(\omega t) \quad (4)$$

As has been discussed repeatedly in the past, the sudden erosion of the safe basin after a saddle connection event can be used as a guide to where transient capsizes will occur [1]. We can use Melnikov's method to derive an approximate boundary for the occurrence of the saddle connection in the (F, ω) parameter [10]. To find an equivalent damping for transient capsizes, we can perform a Melnikov analysis on the 'real' and equivalent systems. It is then possible to choose ζ so that the $F^M(\omega)$ curves (and hence the predicted capsizes domain) are the same for both damping functions.

A simple way to view the Melnikov analysis is as an energy balance over the relevant homoclinic or heteroclinic orbit: for the nonlinearly damped system this gives,

$$\int_{-\infty}^{\infty} b(\dot{x})\dot{x}dt = \int_{-\infty}^{\infty} F \sin(\omega t + t_0)\dot{x}dt \quad (5)$$

where $\dot{x}(t)$ is found for the homoclinic or heteroclinic orbit in the Hamiltonian system and the integrals are taken over this orbit. Rewriting then gives,

$$F^M = \frac{\int_{-\infty}^{\infty} b(\dot{x})\dot{x}dt}{\int_{-\infty}^{\infty} \sin(\omega t + t_0)\dot{x}dt} \quad (6)$$

If we then express $b(\dot{x}) = b_1\dot{x} + b_2|\dot{x}|\dot{x} + b_3\dot{x}^3 + \dots$, (6) can be rewritten in terms of a sum of integrals for each damping term,

$$F^M = \frac{b_1 I_1 + b_2 I_2 + \dots + b_n I_n}{I_F(\omega)} \quad (7)$$

where $I_F(\omega)$ is the denominator of equation (6). The important feature here is that the damping terms have no dependence on forcing frequency.

If we go through the same process for the linearly damped system it is easy to see that the result will be,

$$F^M = \frac{2\zeta I_1}{I_F(\omega)} \quad (8)$$

This means that exactly the same $F^M(\omega)$ curve can be obtained for the linear system, providing:

$$\zeta^M = \frac{b_1 I_1 + b_2 I_2 + \dots + b_n I_n}{2I_1} \quad (9)$$

We have thus defined a Melnikov Equivalent Linear Damping, ζ^M (In [10] this term is defined in a different way). We shall apply this idea now for two example systems. In order to find the Melnikov equivalent damping for a particular system we should calculate the integrals in equation (9). Since each integral is a function of the velocity over the orbit, they depend on the stiffness function $c(x)$. Let us derive ζ^M for two example systems having quadratic (i.e. biased to an extent of having only one-sided escape) and cubic (i.e. symmetric) restoring.

Biased restoring

For this example we take the restoring moment to be $x-x^2$. The first thing to know is an analytical expression for the homoclinic orbit from the saddle point at $x=1$. We locate the saddle connection orbit in the unforced undamped system and then find the energy loss around this orbit. The solution for this homoclinic orbit can be found for example in [11] and is $x(t)=-3/(1+\cosh t)$. Substitution into (9) followed by calculation of the integrals (retaining only up to third order terms in damping) gives the following result,

$$\zeta^M = \frac{1}{2}b_1 + \frac{15}{64}b_2 + \frac{9}{77}b_3 \quad (10)$$

Of course in practical applications we should either use the quadratic or the cubic term in the above expression.

Symmetric restoring

For this example we take the restoring moment to be $x-x^3$. Therefore we are interested in the heteroclinic orbit between the two saddle points at $x = \pm 1$. The solution for the heteroclinic orbit can again be found [12] and is $x(t) = \pm \tanh(t/\sqrt{2})$. Substituting this into (9) and solving the integrals gives,

$$\zeta^M = \frac{1}{2}b_1 + \frac{2\sqrt{2}}{10}b_2 + \frac{6}{35}b_3 \quad (11)$$

3. EXPERIMENTS OF LARGE-ANGLE ROLL AND CAPSIZE

The experiments were conducted in a wave tank of length 8.9m and width 0.585, with a model of length 0.57m. The length of the model is, of course, too small if we intended to predict the behaviour of a specific ship. However, in our case we are only interested in the experimental verification of the nonlinear theory of capsize. Moreover, a model of this size is a great deal easier to position and manipulate than one of larger scale. The water depth was 0.5m, with wave generation provided by a vertical paddle wave maker. A wire mesh was placed in front of the paddle to damp out high frequency 'ripples' on the wave surface. The throw, being the amplitude of the paddle motion, controlled the height of the wave although this was also dependent on the frequency. The wave period was controlled by varying the paddle oscillation frequency. In order to measure the height and frequency of the wave, we employed a wave probe connected to a computer a sampling rate of 30 Hz. The wave probe was positioned 1.5m from the wavemaker and 0.5m in front of the model. The model was free to drift and this led to the encounter frequency varying a small amount, but with the drift speed much lower than the wave celerity this effect was taken to be negligible.

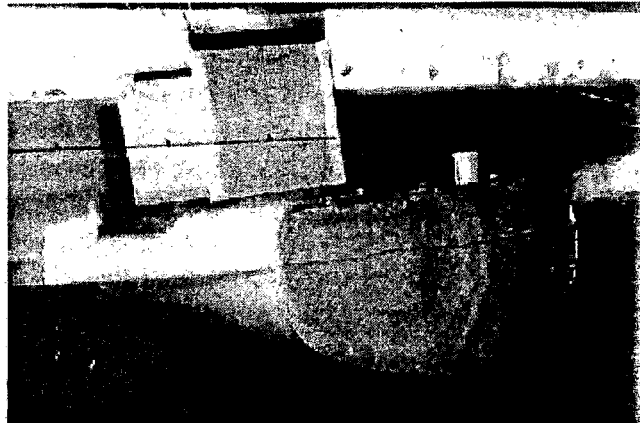


Figure 1: Photograph of model rolling in response to a low amplitude wave.

Some limitations existed in the generation of large amplitude, long period waves and we have considered only deep water conditions with the water depth always at least half the wavelength. The wavelength was generally much larger than the beam. The roll angle was measured with a $\pm 50^\circ$ inclinometer situated inside the model (again sampling at 30 Hz). The inclinometer was tested to ensure that the magnitude of the lateral accelerations likely to occur would not have a significant effect on the measured roll angle. An umbilical cable for data acquisition was held loosely above the model to minimise any effect on the rolling.

We wished to maximise damping of the waves at the beach, thus minimising interference from reflected waves and avoid modulations in the wave amplitude once steady state is reached. When present, such modulations were, however, quite small compared to the steady state wave amplitude. When considering the wave height (or slope) for capsize, we recorded the mean of the steady-state wave while also noting the maximum height achieved.

Model selection

Our primary objective was to derive the capsize boundary on the plane of wave slope against frequency. Hence, we required a design that could be capsized over a range of frequencies for the wave slopes we were able to generate. An appropriate choice was found to be the model design based upon the low freeboard hull used by [5], for which capsize tests had been successfully made. In order to understand better the connections between hull shape and capsize we decided to use a prismatic (2-dimensional) model and thus reduce the number of parameters in the system.

The scale was chosen so that the beam remained small compared to the wavelength up to the highest wave frequencies used. Variation of model parameters was also required and the use of magnetic masses meant that GM and hence natural frequency were easily altered. A question that arose before the tests were made was whether the model should be restrained in certain directions or set free. Ideally, yawing should be restrained. A benefit of the use of a prismatic model was the reduced tendency to yaw. It was also found that by leaving minimal clearance between the ends of the model and the sides of the tank, yaw motion was generally suppressed without contact being made. As a result we were able to conduct the

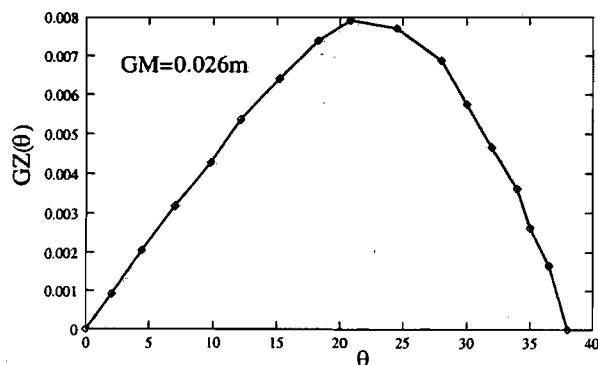


Figure 2: The experimental GZ curve for the model

tests with the model unrestrained. As was discussed in [4], for capsize tests the model should not be restrained in sway because then it cannot follow the motion of the water particles. The magnetic masses were used to 'tune' the natural frequency of the model such that wave frequencies above and below this were available. To a large extent this natural frequency constraint defined the GM for the model which was set to be as low as possible.

For maximum accuracy we performed roll decay and GZ tests to determine $B(\theta')$ and $GZ(\theta)$. The moment of inertia (including added mass) $I + \Delta I$ was derived from the natural frequency. The GZ curve is plotted in figure 2.

Roll damping

To calculate the damping coefficients we performed decay tests with the model conditioned as for the capsize tests. Using an energy balance fitting approach the nonlinear damping coefficients were then estimated. We also used the method

outlined in section 2 to find a value for the Melnikov Equivalent Damping. The damping coefficients are shown in Table 1 below:

Table 1: damping coefficients

ω_n	b_1	b_3	ζ^M (for cubic restoring)
6.7	0.063	0.26	0.077

4. RESONANCE RESPONSE

In order to better characterise the system before conducting the capsizing tests, the resonance response diagram was experimentally derived. This was done by sweeping through a range of frequencies at fixed paddle throw. The chosen position for the magnetic masses set the natural frequency of the model measured as $\omega_f = 6.7\text{s}^{-1}$.

In figure 3 we show a resonance response plot which, with two steady-state solutions existing for the same wave frequencies, displays the nonlinear nature of the system. Also note the shift in the resonance peak to lower frequencies, as expected for a softening system (linear resonance is at $\omega=1$). Note that, since wave slope increases with frequency, the roll amplitude remains large for high ω .

A time series in which the roll motion is knocked from large to small angle roll (and vice versa) is displayed in figure 4. The difficulty with observing steady state motions such as these is that they can only be identified after a number of waves cycles have passed the ship; but at the same time this introduces inaccuracies due to wave reflection. Although some modulation (due to the modulation of the wave) is evident, the existence of two solutions can be seen and the model was knocked between the two types of motion a number of times. As can be seen in figure 3, this behaviour was observed over a range of wave frequencies. Moreover both steady states were robust to perturbations in the forcing (e.g. the reflection induced modulation).

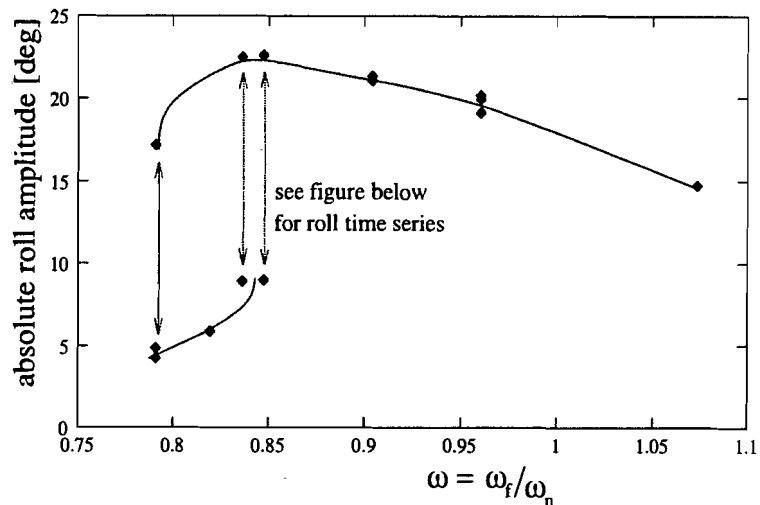


Figure 3: A frequency response diagram, plotted to show the nonlinear nature of the system. Two possible solutions exist just below resonance

It is also worth noting from figure 4 that there is significant bias in the response. This feature is particularly evident in the resonant motion, but was observed throughout the tests. The model itself was set up carefully to be symmetric in its static response and furthermore, when rotated by 180° the bias remained in the same direction, namely towards the wave. Hence, the bias in the response must have been due to asymmetry in the forcing, either from the shape of the waves or second order forces (drift effects). Taken with the effect that even small amounts of bias can have for dynamic stability in the resonance region [13,14], this aspect seems an interesting topic for future research.

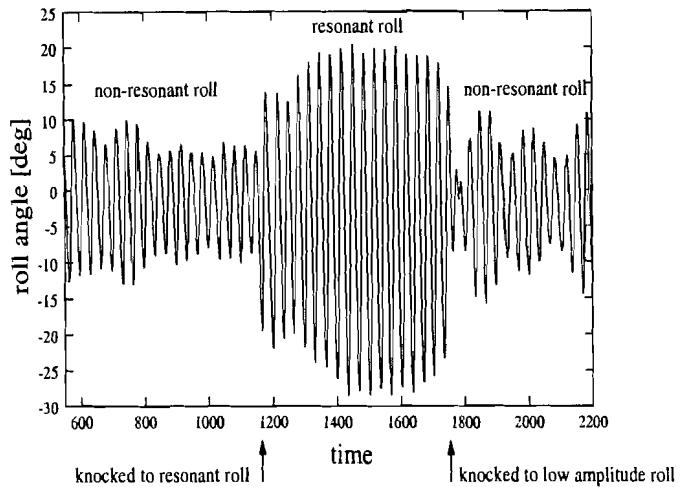


Figure 4: Experimental evidence for two solutions for roll motion. The model was successfully knocked from one to the other a number of times: this plot shows this occurring twice; at $t=1150$ and $t=1750$ (sampling rate, $\Delta t=1/30$ secs). The wave had a mean slope of $Ak=0.11$ and frequency $\omega=5.7s^{-1}$.

Transient capsizing tests

A series of sweeps through frequency were made for fixed paddle throws with the model placed at the same distance from the wavemaker at the beginning of each run. As for the resonance response test, the natural frequency was set to be $\omega_f=6.7s^{-1}$. Note that as frequency was increased, the wave height (and slope) also increased. For each wavemaker throw and frequency we recorded whether capsizing had occurred. Then from the wave data we deduced the exact frequency and amplitude.

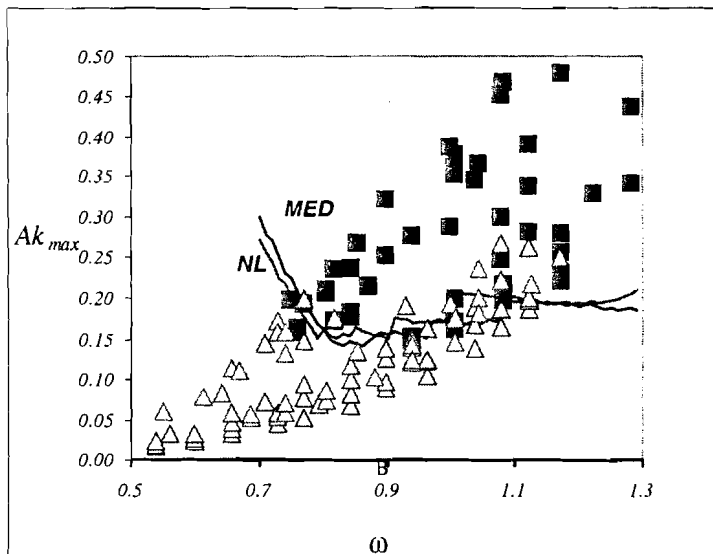


Figure 5: Transient capsizing diagram. Shown are the transient capsizing predictions from numerical simulations using full nonlinear damping (NL) and the Melnikov Equivalent Damping (MED).

In figure 5 the capsizing results are plotted against the simulated transient capsizing boundary for nonlinear (NL) and “Melnikov-equivalent” linear damping (MED). This boundary is generated by considering a ship at rest in still water with the wave forcing ‘turned on’ at a certain amplitude.

Due to the difficulty in assigning a steady state wave amplitude with the modulation present, we have considered a transient measure of amplitude, the maximum value of A . The realisation of this maximum

represents a hard capsizability test for the model. The amplitude is increased in small steps from zero, at a particular frequency, until capsize (defined as roll beyond θ_V) is detected whereupon a point on the transient capsize boundary is plotted. Since only one initial condition (static rest) is considered for each wave slope and frequency, the use of this boundary as a good lower bound for capsize relies upon the concept of the Dover cliff [15]. The essence of this phenomenon is that, in a certain parameter range, for a small increase in wave slope there is a dramatic reduction in the 'safe basin' (the number of initial conditions that do not lead to capsize). As a result we need only test for one starting condition. Of course there is a possibility that the starting condition chosen is a freak safe one but with small increases in Ak each time it is highly unlikely that this will occur at the next step.

While the conditions for capsize are found to agree well with the numerical prediction, note that there exist non-capsizing results for wave slopes higher than some capsizing tests. The reason for this lies in the importance of initial conditions. For the numerical 'test' the erosion of the safe basin with rising wave slope (the Dover cliff phenomenon) [15] implies that the choice of initial condition for a capsize test is not significant. However, for our experiments we have found that this is not always the case.

Initial conditions

It was found that near the capsize boundary, variation of the initial paddle position had an effect on capsize. In effect, the difference in the wave build up (determined by the paddle start position) was enough to cause the model to end up in a different basin of attraction (safe or capsizing). This behaviour can be seen in figure 5, where capsizing and non-capsizing tests were observed for the same wave forcing (particularly for $0.9 < \omega < 1.2$). Since the measured wave heights were a maximum value for a modulating wave, there is some variation in Ak , even though the wavemaker control settings were the same.

In figure 6, the time series of a test repeated with a different paddle start position is shown. Note that, because the wave probe was in front of the model (with respect to the wave) the roll is delayed with respect to the wave. This is enhanced by the slow drift of the model. The important difference is in the wave build up. In this case an initial trough causes capsize but if the first wave is a crest then steady-state roll is the result. This sensitivity to the wave build up was consistently repeated and the same dependence seen for a particular slope and frequency.

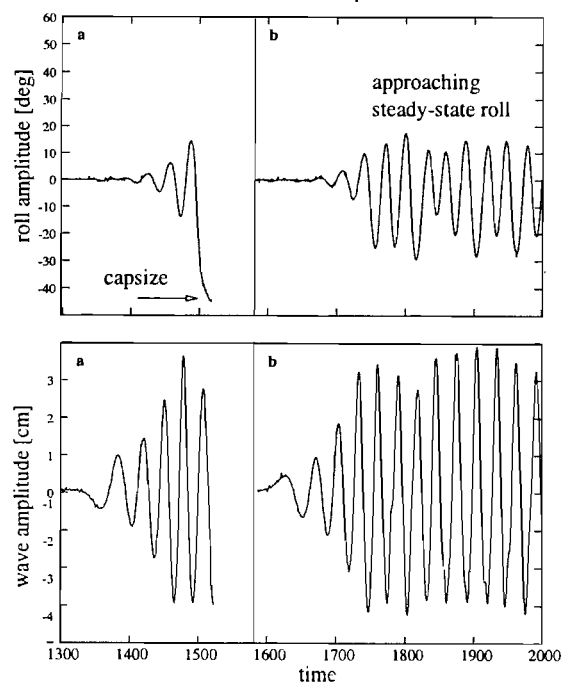


Figure 6: The first test, (a), leads to capsize while (b) does not. The only difference is the initial conditions; the wave forcing has a phase shift of half a period between each test.

As a further illustration of the bias present, the model always capsized towards the wave. In a short test in which we added a small bias on the side away from the wave it was found that a static heel of only a few degrees was enough to cause capsize to occur in the direction of the bias. Again this supports theoretical studies which predict that symmetry breaking (even by a small bias) either inherent in the model, or induced by the wave forcing, has a profound effect on capsize.

5. CONCLUDING REMARKS

In this paper we derive a new equivalent linear damping concept, based on a capsize criterion. Using Melnikov's approach we have derived an expression for a cubic or a quadratic GZ fit and we tested these against the experimental capsize results described in the second part of the paper. In this series of tests we have initiated the process of providing experimental evidence for the complex nonlinear phenomena which have been theoretically predicted to be linked to capsize. Two stable oscillations were found to exist for frequency ratios of $0.8 < \omega < 0.85$ ($Ak \cong 0.12$). Jumps between such oscillations proved easy to achieve experimentally (a light tap was typically enough).

An important feature observed in the tests was the presence of wave-induced bias. This took the form of a reflective static heel angle of approximately 2° to 3° . Taken with the sensitivity of ship capsize resistance to a bias in the ship [13,14] the causes and effects of this bias certainly merit further investigation.

The capsize tests were compared with a numerically generated 'transient capsize line'. This involves considering the capsize of the ship from one initial condition, given the sudden onset of a wave of a certain amplitude and frequency. Our tests represent a first step and there is clearly a need for further work on this front. Finally we have presented some data demonstrating the importance of considering initial conditions when testing for capsize. We should also note that throughout these experiments all tests were carried out at least twice (sometimes many more) for each condition in order to establish the repeatability of the outcome.

ACKNOWLEDGMENTS

These experiments have been supported by the UK Defence Evaluation and Research Agency with a special grant as part of a long-standing project on ship capsize, headed by Prof. J.M.T. Thompson of UCL. We also acknowledge several discussions with Prof. J.M.T. Thompson and Prof. S.R. Bishop of UCL as well as P. Crossland and M. Johnson of DERA. The capsize tests were conducted with the assistance of V. Chan who is a UCL student.

REFERENCES

1. Thompson, J.M.T. (1997) Designing against capsizes in beam seas: Recent advances and new insights. *Applied Mechanics Reviews* **50**, 307-325.
2. Kan, M., Saruta, T. & Taguchi, H. (1991) Capsizing of a ship in quartering waves, *Naval Architecture and Ocean Engineering*, **29**, 49-60.
3. Nayfeh, A.H. & Sanchez, N.E. (1988) Stability and Complicated Rolling Responses of Ships in Regular Beam Waves. *International Shipbuilding Progress* **37(412)**, 331-352.
4. Spyrou, K.J. (1998) Ship capsizes assessment and nonlinear dynamics. In *Proceedings of the Fourth International Workshop on Theoretical Advances in Ship Stability and Practical Impact*, St John's, Newfoundland, Canada, September.
5. Wright, J.H.G. & Marshfield, W.B. (1980) Ship roll response and capsizes behaviour in beam seas. *Transactions of the Royal Institute of Naval Architects* **122**, 129-148.
6. Contento, G. & Francescutto, A. (1997) Intact stability in beam seas: Mathematical modelling of large amplitude motion. In *Proceedings of the 3rd International Workshop on Theoretical Advances in Ship Stability and Operational Safety of Ships*, Hersonissos, Greece, pp. 59-68.
7. Dalzell, J.F. (1978) A note on the form of ship roll damping, *Journal of Ship Research*, **22(3)**, 178-185.
8. Haddara, M.R. & Bennet, P. (1989). A study of the angle dependence of ship roll damping, *Ocean Engineering*, **16**, 411-427.
9. Vassilopoulos, L. (1971). Ship rolling at zero speed in random beam seas with nonlinear damping and restoration, *Journal of Ship Research*, **15(4)**.
10. Bikdash, M., Balachandran, B. & Nayfeh, A.H. (1994). Melnikov analysis for a ship with a general roll-damping model. *Nonlinear Dynamics* **6**, 101-124
11. Thompson, J.M.T. (1989) Chaotic phenomena triggering the escape from a potential well. *Proceedings of the Royal Society London, A* **421**, 195-225.

12. Nayfeh, A.H. & Balachandran, B. (1995) *Applied Nonlinear Dynamics*. New York: Wiley.
13. Macmaster, A.G. & Thompson, J.M.T. (1994) Wave tank testing and the capsizability of hulls. *Proceedings of the Royal Society London* **446**, 217-232.
14. Cotton, B., Bishop, S.R. & Thompson, J.M.T. (1997) Sensitivity of capsizing to a symmetry breaking bias. In *Proceedings of the Second Workshop on Stability and Operational Safety of Ships*, Osaka University, Japan, October.
15. Thompson, J.M.T., Rainey, R.C.T. & Soliman, M.S. (1990) Ship stability criteria based on chaotic transients from incursive fractals. *Philosophical Transactions of the Royal Society of London*. **332**, 149-167.